

Light-Driven Water Splitting by a Covalently Linked Ruthenium-Based Chromophore–Catalyst Assembly

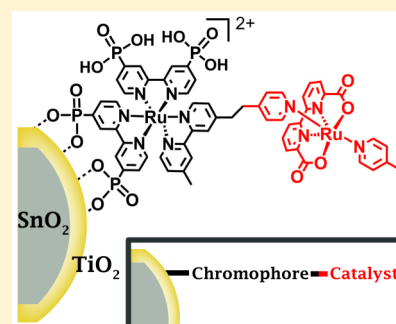
Benjamin D. Sherman,[†] Yan Xie,[‡] Matthew V. Sheridan,[†] Degao Wang,[†] David W. Shaffer,[‡] Thomas J. Meyer,[†] and Javier J. Concepcion^{*†‡}

[†]Department of Chemistry, University of North Carolina Chapel Hill, Chapel Hill, North Carolina 27599, United States

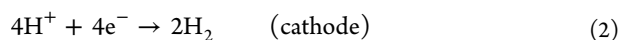
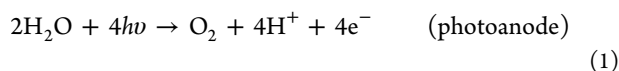
[‡]Chemistry Division, Brookhaven National Laboratory, Upton, New York 11973, United States

S Supporting Information

ABSTRACT: The preparation and characterization of new Ru(II) polypyridyl-based chromophore–catalyst assemblies, $[(4,4'-\text{PO}_3\text{H}_2\text{-bpy})_2\text{Ru}(4\text{-Mebpy-4'-epic})\text{-Ru}(\text{bda})(\text{pic})]^{2+}$ (**1**, bpy = 2,2'-bipyridine; 4-Mebpy-4'-epic = 4-(4-methylbipyridin-4'-yl-ethyl)-pyridine; bda = 2,2'-bipyridine-6,6'-dicarboxylate; pic = 4-picoline), and $[(\text{bpy})_2\text{Ru}(4\text{-Mebpy-4'-epic})\text{Ru}(\text{bda})(\text{pic})]^{2+}$ (**1'**) are described, as is the application of **1** in a dye-sensitized photoelectrosynthesis cell (DSPEC) for solar water splitting. On $\text{SnO}_2/\text{TiO}_2$ core–shell electrodes in a DSPEC configuration with a Pt cathode, the chromophore–catalyst assembly undergoes light-driven water oxidation at pH 5.7 in a 0.1 M acetate buffer, 0.5 M in NaClO_4 . With illumination by a 100 mW cm^{-2} white light source, photocurrents of $\sim 0.85 \text{ mA cm}^{-2}$ were observed after 30 s under a 0.1 V vs Ag/AgCl applied bias with a faradaic efficiency for O_2 production of 74% measured over a 5 min illumination period.

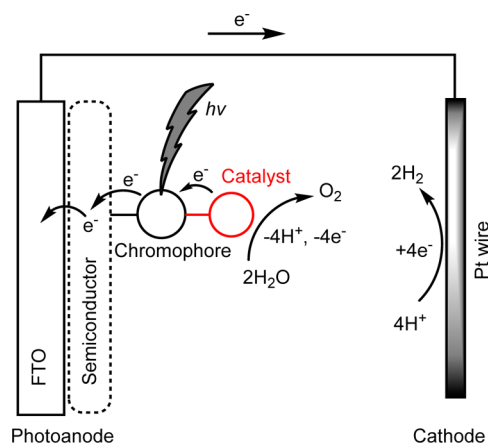


Photoelectrochemical water splitting and the production of fuels with energy harnessed from sunlight (“solar fuels”) will likely play an important role in our energy future.^{1,2} In this approach, energy from solar radiation drives production of a fuel such as H_2 , CO, or CH_4 , coupled with the oxidation of water to O_2 .³ Dye-sensitized photoelectrosynthesis cells (DSPECs) have been shown to carry out solar-driven water splitting, and the improvement of this technology has focused on the development of higher-performing photoanodes.^{4–6} A DSPEC photoanode integrates a nanoparticulate wide-band-gap n-type semiconductor oxide film, such as *nano* TiO_2 , with a molecular chromophore–catalyst assembly for carrying out light absorption and catalyzing the oxidation of water to O_2 (eq 1).



As illustrated in Scheme 1, following light absorption by the surface-attached chromophore moiety, electron transfer from the excited state of the chromophore results in a reductive equivalent at the conduction band potential of the oxide. Intra-assembly electron transfer from the catalyst component to the photo-oxidized chromophore, re-forming the ground-state chromophore, initiates the process of the $4\text{e}^-/4\text{H}^+$ oxidation of water. In this sequence, the energy of the molecular excited state of the chromophore is sequentially converted to

Scheme 1. Diagram of a Dye-Sensitized Photoelectrosynthesis Cell (DSPEC) for Solar Water Splitting



transiently stored redox energy in the form of the reduced semiconductor oxide and the oxidized state of the catalyst.

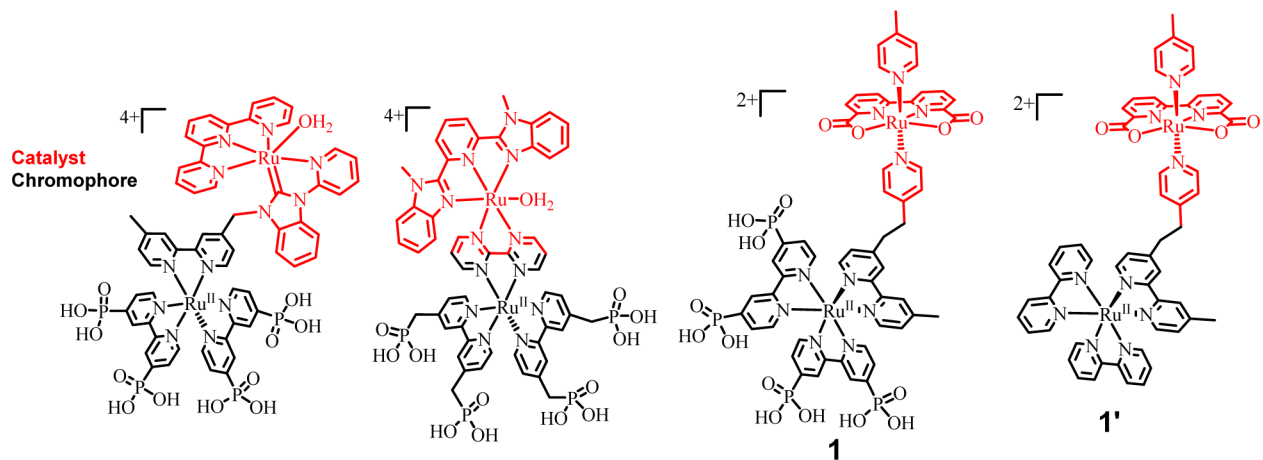
Diffusion of injected electrons in the semiconductor film to the transparent conducting oxide (fluorine-doped tin oxide

Received: December 6, 2016

Accepted: December 9, 2016

Published: December 9, 2016

Scheme 2. Examples of Ruthenium-Based Covalently Linked Chromophore–Catalyst Assemblies



(FTO) used here) and electron transfer to H^+ at the cathode result in the production of H_2 . Driving proton reduction to H_2 at the cathode, when connected to a TiO_2 photoanode, requires an external bias due to the inability of the TiO_2 –dye interface to support a sufficiently negative potential despite the more negative conduction band potential of anatase TiO_2 as compared to the H^+/H_2 potential.⁷ The needed bias can be supplied by an external source (potentiostat), dye-sensitized solar cell (DSSC) wired in series,^{8,9} or an integrated photocathode.^{10,11}

A variety of chromophore–catalyst assemblies have been investigated for DSPEC applications.¹² The simplest assembly strategy is co-loading the chromophore and catalyst on the oxide surface with chromophore injection followed by cross-surface electron transfer activation of the catalyst.^{13–15} Though a straightforward approach, this strategy provides little spatial separation between the catalyst and oxide surface, resulting in minimal inhibition of back electron transfer from the oxide to the oxidized catalyst. In another assembly strategy, Zr(IV) –phosphonate bridging has been used to link a chromophore and catalyst on oxide surfaces.^{16–18} While establishing greater distance between the oxide surface and catalyst, this approach relies on a hydrolytically unstable connection. Covalently linked assemblies, by comparison, have the advantage of providing a chemically stable linkage between the chromophore and catalyst while also introducing a spatially controllable separation distance for ameliorating the effects of back electron transfer.^{5,19–25} The obvious value of this approach is offset by formidable synthetic challenges that arise from preparing such assemblies.

We describe here, for the first time, an assembly designed for attachment to an oxide surface in which a $[\text{Ru}(\text{bda})(\text{L})_2]$ (bda = 2,2′-bipyridine-6,6′-dicarboxylate, L = a neutral donor ligand such as pyridine or isoquinoline) catalyst is incorporated into the covalently linked assembly, $[(4,4′\text{-PO}_3\text{H}_2\text{-bpy})_2\text{Ru}(4\text{-Mebpy-4′-epic})\text{Ru}(\text{bda})(\text{pic})]^{2+}$ (**1**, 4,4′- $\text{PO}_3\text{H}_2\text{-bpy}$ = 4,4′-phosphonic acid-2,2′-bipyridine; 4-Mebpy-4′-epic = 4-(4-methylbipyridin-4′-yl-ethyl)-pyridine; pic = 4-picoline), with a Ru(II) polypyridyl chromophore (see Scheme 2). For comparison purposes, we also describe the nonphosphonated assembly **1′** ($[(\text{bpy})_2\text{Ru}(4\text{-Mebpy-4′-epic})\text{Ru}(\text{bda})(\text{pic})]^{2+}$). The latter is used as the solution analogue of **1**. A series of reports have appeared on visible DSPEC water splitting based on $[\text{Ru}(\text{bda})(\text{L})_2]$ water oxidation catalysts by Sun and co-

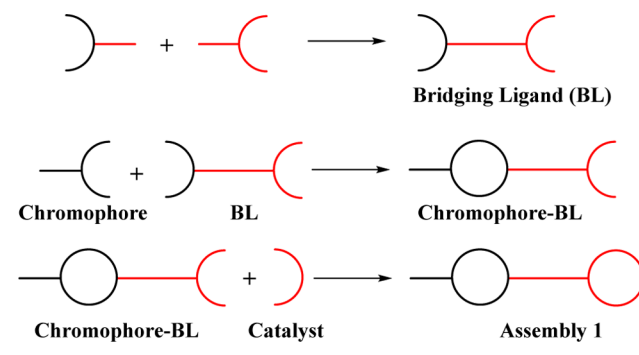
workers,²⁶ who have integrated $[\text{Ru}(\text{bda})(\text{L})_2]$ catalysts with polypyridyl chromophores in a variety of applications.^{14,27}

Low overpotentials and high rates of water oxidation by the family of $[\text{Ru}(\text{bda})(\text{L})_2]$ catalysts make them ideal for use in light-driven DSPEC applications with Ru(II) polypyridyl chromophores. The potential for the $[\text{Ru}(\text{bpy})_3]^{3+/2+}$ couple is sufficient to drive $[\text{Ru}(\text{bda})(\text{L})_2]$ -based water oxidation catalytic cycles to completion with the reduction potential for the $\text{Ru}^{\text{V/IV}}$ couple typically ~ 0.9 V vs Ag/AgCl at pH 7.^{28,29}

We describe here the synthesis, electrochemistry, and photoelectrochemistry of **1** on nanoparticle TiO_2 and $\text{SnO}_2/\text{TiO}_2$ core–shell films, the latter used for light-driven water oxidation at pH 5.7 in acetate buffer. As found in previous studies, the core–shell electrodes provide superior device performance in both the magnitude of photocurrents and faradaic efficiency (FE) for O_2 production.⁴ Under simulated solar illumination (100 mW cm^{-2} white light), photocurrents were observed at a magnitude of 0.15 mA cm^{-2} on TiO_2 and 0.85 mA cm^{-2} on $\text{SnO}_2/\text{TiO}_2$ core–shell electrodes after 30 s of light exposure.

Assembly **1** was prepared following a modular approach, Scheme 3 (see the Supporting Information for details). It

Scheme 3. Modular Synthetic Approach



involved the synthesis of the bridge followed by selective binding of the bidentate side of the bridge to the chromophore. The catalyst was incorporated in the final step using the dangling pyridine for catalyst binding. The synthesis of the bridging ligand was achieved by a coupling reaction between 4-picoline and 4-bromomethyl-4′-methyl-2,2′-bipyridine. The bridging ligand was then reacted with $[\text{Ru}(4,4′\text{-(PO}_3\text{H}_2)_2\text{-bpy})_2\text{Cl}_2]$ in a microwave reactor to give a chromophore with a

saturated aliphatic linker bridge with a dangling pyridine for catalyst binding and phosphonic acid groups for surface anchoring. Reaction of the dangling pyridine with the catalyst precursor $[(\text{bda})\text{Ru}(\text{pic})(\text{DMSO})]$ afforded assembly **1** after purification by column chromatography on Sephadex LH-20. The analogous assembly without phosphonate groups, assembly **1'**, was prepared following a similar procedure. The additive features of the different “modules” were corroborated by comparison of the absorption spectra of the assembly with the sum of the absorption spectra of the different modules. For spectroscopic comparison, $[\text{Ru}(4,4'\text{-Me-bpy})(4,4'\text{-PO}_3\text{H}_2\text{-bpy})_2]^{2+}$ ($4,4'\text{-Me-bpy} = 4,4'\text{-methyl-2,2'-bipyridine}$) was used as the model chromophore, $[\text{Ru}(\text{bda})(\text{pic})_2]$ was used as the catalyst model for assembly **1** (Figure S11), and $[\text{Ru}(4,4'\text{-Me-bpy})(\text{bpy})_2]^{2+}$ and $[\text{Ru}(\text{bda})(\text{pic})_2]$ were used as the chromophore and catalyst models for **1'** (Figure S9). The aliphatic nature of the linker ensures the retention of the individual properties of the different modules, with the nature of the bridge resulting in minimal through-bridge coupling between the chromophore and catalyst.

Cyclic voltammograms (CVs) of the parent chromophore and catalyst components of **1** are shown in Figure 1. The CVs

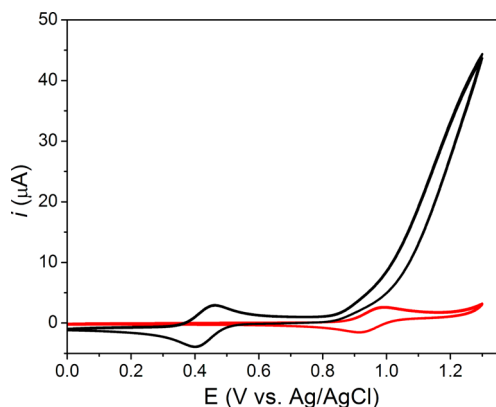


Figure 1. Cyclic voltammograms (CVs) of 0.5 mM $[\text{Ru}(4,4'\text{-Me-bpy})(4,4'\text{-PO}_3\text{H}_2\text{-bpy})_2]\text{Cl}_2$ (red) and $[\text{Ru}(\text{bda})(\text{pic})_2]$ (black) in pH 5.7, 0.1 M acetate buffer, 0.5 M in NaClO_4 . The voltammograms were recorded with a BDDE working electrode with a scan rate of 50 mV s^{-1} .

of the $[\text{Ru}(4,4'\text{-Me-bpy})(4,4'\text{-PO}_3\text{H}_2\text{-bpy})_2]^{2+}$ chromophore and $[\text{Ru}(\text{bda})(\text{pic})_2]$ catalyst were measured at pH 5.7 with a boron-doped diamond electrode (BDDE). The onset of catalytic current occurs at $\sim 0.85 \text{ V}$ vs Ag/AgCl for $[\text{Ru}(\text{bda})(\text{pic})_2]$ (black) and the $\text{Ru}^{\text{III/II}}$ couple of the $[\text{Ru}(4,4'\text{-Me-bpy})(4,4'\text{-PO}_3\text{H}_2\text{-bpy})_2]$ chromophore appears at 0.95 V vs Ag/AgCl. The CVs illustrate the catalytic reactivity of $[\text{Ru}(\text{bda})(\text{pic})_2]$ toward water oxidation and the ability of the $\text{Ru}(\text{III})$ state of the chromophore to provide sufficient overpotential to oxidize the catalyst and drive water oxidation catalysis.

Figure 2 compares CVs of **1** bound to a planar FTO electrode (FTO-1) to an unmodified FTO electrode and a FTO electrode modified with $[\text{Ru}(4,4'\text{-PO}_3\text{H}_2\text{-bpy})(\text{bpy})_2]^{2+}$ (RuP^{2+}). In the CV of FTO-1, the $\text{Ru}^{\text{III/II}}$ couple is observed at 0.45 V vs Ag/AgCl, with an anodic current increase at $\sim 0.75 \text{ V}$ vs Ag/AgCl consistent with oxidation of the catalyst from Ru^{III} to Ru^{IV} . Catalytic current due to water oxidation by the Ru^{V} form of the catalyst is initiated at $\sim 0.85 \text{ V}$ vs Ag/AgCl with a peak in the current response at $E_{\text{p,cat}} = 1.02 \text{ V}$ vs Ag/AgCl.

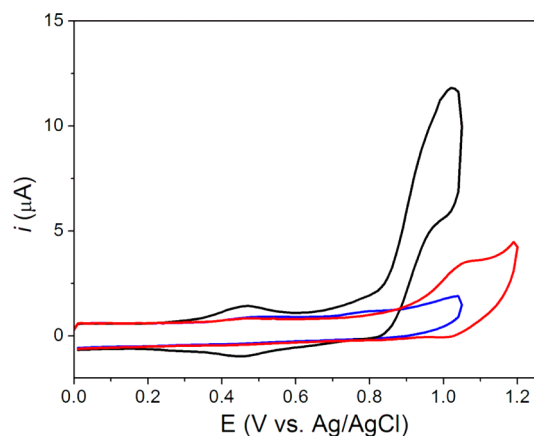


Figure 2. CVs measured at a 1 cm^2 FTO electrode modified with **1** (black), RuP^{2+} (red), or an unmodified FTO electrode (blue) in pH 5.7, 0.1 M acetate buffer with 0.5 M NaClO_4 . The voltammograms were recorded at a scan rate of 25 mV s^{-1} .

These observations are consistent with the potentials observed for the chromophore and catalyst components in solution, as shown in Figure 1. The $\text{Ru}^{\text{III/II}}$ couple for RuP^{2+} on FTO in Figure 2 appears at 1.04 V vs Ag/AgCl, sufficiently positive to oxidize the catalyst to the Ru^{V} state and initiate water oxidation. The CV of **1** at a planar FTO electrode at pH 1 is shown in Figure S3, and CVs and square-wave voltammograms of **1'**, $[\text{Ru}(4,4'\text{-Me-bpy})(\text{bpy})_2]^{2+}$, and $[\text{Ru}(\text{bda})(\text{pic})_2]$ in solution at pH 1 are shown in Figures S4–S6. The data demonstrate the additive nature of the redox features of the assembly as compared to that of the individual components. Comparison of UV–vis spectra of **1**, $[\text{Ru}(4,4'\text{-PO}_3\text{H}_2\text{-bpy})(\text{bpy})_2]^{2+}$, and $[\text{Ru}(\text{bda})(\text{pic})_2]$ (Figure S11) and **1'**, $[\text{Ru}(4,4'\text{-Me-bpy})(\text{bpy})_2]^{2+}$, and $[\text{Ru}(\text{bda})(\text{pic})_2]$ (Figure S9) complement the CV data and demonstrates that the chromophore and catalyst moieties maintain their individual electrochemical and spectral properties in **1** and **1'**.

Current density vs time ($j-t$) traces under dark/light cycling conditions are shown in Figure 3 for assembly **1** on both TiO_2

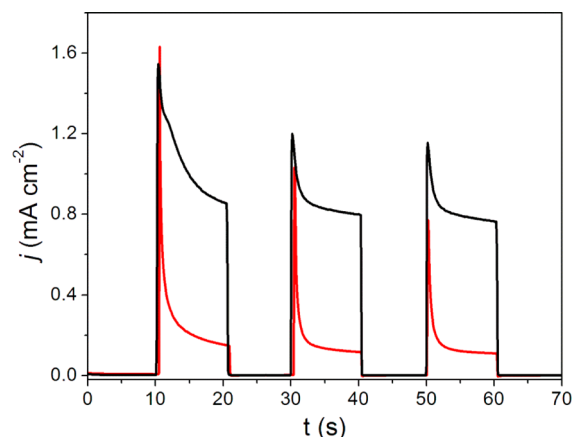


Figure 3. Current density vs time traces measured with $\text{FTO}/\text{SnO}_2/\text{TiO}_2\text{-1}$ (1 cm^2 , black) and $\text{FTO}/\text{TiO}_2\text{-1}$ (1 cm^2 , red) photoanodes at pH 5.7 with 0.1 M acetate buffer and 0.5 M in NaClO_4 . The current traces were recorded under an applied bias of 0.1 V vs Ag/AgCl, and samples underwent sequential 10 s dark/light cycles during the measurement. Illumination was supplied with a white light source at an intensity of 100 mW cm^{-2} .

(FTO|TiO₂|I-1) and the SnO₂/TiO₂ core–shell (FTO|SnO₂/TiO₂|I-1) electrodes. The experiments were conducted with a white light source in pH 5.7 solution with 0.1 M acetate buffer and 0.5 M in NaClO₄. In earlier experiments, significant current enhancements have been observed using core–shell electrodes as compared to TiO₂.⁴ The improved activity arises from injection and rapid electron transfer through the TiO₂ shell to the SnO₂ core with back electron transfer inhibited by a ~0.4 V barrier established by the difference in conduction band potentials between the oxides.^{30,31}

For assembly 1, comparison of photocurrent levels between electrodes yields an enhancement of ~6X for the core–shell electrodes with currents of 0.85 mA cm⁻² as compared to 0.15 mA cm⁻² for TiO₂ after 30 s of illumination. The latter result is consistent with earlier reports for [Ru(bda)(L)₂]-based assemblies for light-driven water splitting on TiO₂.^{25,32} Linear sweep voltammograms (LSVs) for the two electrodes under dark and light conditions are shown in Figure S1. These measurements reveal a more positive potential for the point of zero current consistent with the more positive conduction band potential of SnO₂ as compared with that of TiO₂.

A collector–generator (C–G) dual working electrode method³³ was used to examine light-driven O₂ production at both FTO|TiO₂|I-1 and FTO|SnO₂/TiO₂|I-1 electrodes (Figure S2). The C–G technique has proven to be a convenient, straightforward method for O₂ analysis in both electrochemical^{34,35} and photochemical water oxidation.^{36,37} Application of this technique gave FEs of 74% for FTO|SnO₂/TiO₂|I-1 and 30% for FTO|TiO₂|I-1. O₂ production was also measured using a Clark-type oxygen sensor, which confirmed the C–G results and gave a FE of 71% for FTO|SnO₂/TiO₂|I-1. The details and results of this redundant experiment are provided in the Supporting Information (Figure S12). The exact mechanism leading to the improved O₂ yield of the core–shell photoanode is currently under investigation. A possible reason for this observed behavior may lie in the improved ability of the core–shell interface to support the accumulation of multiple oxidative equivalents. This could lead to a greater portion of the photogenerated holes contributing to the 4 e⁻/4 H⁺ process of water oxidation as opposed to other nonproductive oxidative processes, with the latter dominating on TiO₂.

Our results are important in describing, for the first time, a covalently linked chromophore–catalyst assembly incorporating a [Ru(bda)(L)₂]-type catalyst that performs both electrochemical and photoelectrochemical water oxidation catalysis on oxide surfaces. The modular synthetic approach used here allows for individual tuning of the different functions (light absorption, redox potential of the chromophore, catalytic activity, etc.) before incorporation of the different components into covalently linked assemblies. Comparison of photocurrent levels and FEs for O₂ provide an additional example of the value of the oxide core–shell configuration in achieving both higher photocurrent densities and FEs for O₂ evolution. Further studies of the covalently linked assembly-based DSPEC are underway.

■ ASSOCIATED CONTENT

Supporting Information

The Supporting Information is available free of charge on the ACS Publications website at DOI: 10.1021/acsenergylett.6b00661.

Experimental details, synthetic procedures, and characterization of compounds and intermediates, cyclic voltammograms, collector–generator data, and UV–vis spectra (PDF)

■ AUTHOR INFORMATION

Corresponding Author

*E-mail: jconcepc@bnl.gov.

ORCID

Benjamin D. Sherman: 0000-0001-9571-5065

David W. Shaffer: 0000-0002-8807-1617

Notes

The authors declare no competing financial interest.

■ ACKNOWLEDGMENTS

Electrochemical and photoelectrochemical studies were carried out at UNC (B.D.S, M.V.S., and D.W.) supported by the UNC EFRC Center for Solar Fuels, an Energy Frontier Research Center funded by the U.S. Department of Energy, Office of Science, Office of Basic Energy Sciences, under Award No. DE-SC0001011. Synthesis and characterization of all compounds and spectroscopic studies were carried out at Brookhaven National Laboratory (Y.X. and D.W.S.) supported by the U.S. Department of Energy, Office of Science, Division of Chemical Sciences, Geosciences, & Biosciences, Office of Basic Energy Sciences under Contract DE-SC00112704.

■ REFERENCES

- (1) Walter, M. G.; Warren, E. L.; McKone, J. R.; Boettcher, S. W.; Mi, Q.; Santori, E. A.; Lewis, N. S. Solar Water Splitting Cells. *Chem. Rev.* **2010**, *110*, 6446–6473.
- (2) House, R. L.; Iha, N. Y. M.; Coppo, R. L.; Alibabaei, L.; Sherman, B. D.; Kang, P.; Brennaman, M. K.; Hoertz, P. G.; Meyer, T. J. Artificial Photosynthesis: Where are we Now? Where can we Go? *J. Photochem. Photobiol., C* **2015**, *25*, 32–45.
- (3) Blakemore, J. D.; Crabtree, R. H.; Brudvig, G. W. Molecular Catalysts for Water Oxidation. *Chem. Rev.* **2015**, *115*, 12974–13005.
- (4) Sherman, B. D.; Ashford, D. L.; Lapidus, A. M.; Sheridan, M. V.; Wee, K. R.; Meyer, T. J. Light-Driven Water Splitting with a Molecular Electroassembly-Based Core/Shell Photoanode. *J. Phys. Chem. Lett.* **2015**, *6*, 3213–3217.
- (5) Alibabaei, L.; Sherman, B. D.; Norris, M. R.; Brennaman, M. K.; Meyer, T. J. Visible Photoelectrochemical Water Splitting into H₂ and O₂ in a Dye-Sensitized Photoelectrosynthesis Cell. *Proc. Natl. Acad. Sci. U. S. A.* **2015**, *112*, 5899–5902.
- (6) Swierk, J. R.; Mallouk, T. E. Design and Development of Photoanodes for Water-Splitting Dye-Sensitized Photoelectrochemical Cells. *Chem. Soc. Rev.* **2013**, *42*, 2357–2387.
- (7) Hagfeldt, A.; Graetzel, M. Light-Induced Redox Reactions in Nanocrystalline Systems. *Chem. Rev.* **1995**, *95*, 49–68.
- (8) Sherman, B. D.; Bergkamp, J. J.; Brown, C. L.; Moore, A. L.; Gust, D.; Moore, T. A. A Tandem Dye-Sensitized Photoelectrochemical Cell for Light Driven Hydrogen Production. *Energy Environ. Sci.* **2016**, *9*, 1812.
- (9) Brillet, J.; Yum, J. H.; Cornuz, M.; Hisatomi, T.; Solarska, R.; Augustynski, J.; Graetzel, M.; Sivula, K. Highly Efficient Water Splitting by a Dual-Absorber Tandem Cell. *Nat. Photonics* **2012**, *6*, 824–828.
- (10) Li, F.; Fan, K.; Xu, B.; Gabrielsson, E.; Daniel, Q.; Li, L.; Sun, L. Organic Dye-Sensitized Tandem Photoelectrochemical Cell for Light Driven Total Water Splitting. *J. Am. Chem. Soc.* **2015**, *137*, 9153–9159.
- (11) Odobel, F.; Le Pleux, L. c.; Pellegrin, Y.; Blart, E. New Photovoltaic Devices Based on the Sensitization of P-Type Semiconductors: Challenges and Opportunities. *Acc. Chem. Res.* **2010**, *43*, 1063–1071.

- (12) Ashford, D. L.; Gish, M. K.; Vannucci, A. K.; Brennaman, M. K.; Templeton, J. L.; Papanikolas, J. M.; Meyer, T. J. Molecular Chromophore–Catalyst Assemblies for Solar Fuel Applications. *Chem. Rev.* **2015**, *115*, 13006–13049.
- (13) Sheridan, M. V.; Sherman, B. D.; Coppo, R. L.; Wang, D.; Marquard, S. L.; Wee, K. R.; Murakami Iha, N. Y.; Meyer, T. J. Evaluation of Chromophore and Assembly Design in Light-Driven Water Splitting with a Molecular Water Oxidation Catalyst. *ACS Energy Lett.* **2016**, *1*, 231–236.
- (14) Gao, Y.; Ding, X.; Liu, J.; Wang, L.; Lu, Z.; Li, L.; Sun, L. Visible Light Driven Water Splitting in a Molecular Device with Unprecedentedly High Photocurrent Density. *J. Am. Chem. Soc.* **2013**, *135*, 4219–4222.
- (15) Zhao, Y.; Swierk, J. R.; Megiatto, J. D.; Sherman, B.; Youngblood, W. J.; Qin, D.; Lentz, D. M.; Moore, A. L.; Moore, T. A.; Gust, D.; Mallouk, T. E. Improving the Efficiency of Water Splitting in Dye-Sensitized Solar Cells by using a Biomimetic Electron Transfer Mediator. *Proc. Natl. Acad. Sci. U. S. A.* **2012**, *109*, 15612–15616.
- (16) Wang, J. C.; Murphy, I. A.; Hanson, K. Modulating Electron Transfer Dynamics at Dye–Semiconductor Interfaces Via Self-Assembled Bilayers. *J. Phys. Chem. C* **2015**, *119*, 3502–3508.
- (17) Ding, X.; Gao, Y.; Zhang, L.; Yu, Z.; Liu, J.; Sun, L. Visible Light-Driven Water Splitting in Photoelectrochemical Cells with Supramolecular Catalysts on Photoanodes. *ACS Catal.* **2014**, *4*, 2347–2350.
- (18) Hanson, K.; Torelli, D. A.; Vannucci, A. K.; Brennaman, M. K.; Luo, H.; Alibabaei, L.; Song, W.; Ashford, D. L.; Norris, M. R.; Glasson, C. R. K.; Concepcion, J. J.; Meyer, T. J. Self-Assembled Bilayer Films of Ruthenium(II)/Polypyridyl Complexes through Layer-by-Layer Deposition on Nanostructured Metal Oxides. *Angew. Chem., Int. Ed.* **2012**, *51*, 12782–12785.
- (19) Ashford, D. L.; Song, W.; Concepcion, J. J.; Glasson, C. R. K.; Brennaman, M. K.; Norris, M. R.; Fang, Z.; Templeton, J. L.; Meyer, T. J. Photoinduced Electron Transfer in a Chromophore–Catalyst Assembly Anchored to TiO₂. *J. Am. Chem. Soc.* **2012**, *134*, 19189–19198.
- (20) Norris, M. R.; Concepcion, J. J.; Fang, Z.; Templeton, J. L.; Meyer, T. J. Low-Overpotential Water Oxidation by a Surface-Bound Ruthenium-Chromophore–Ruthenium-Catalyst Assembly. *Angew. Chem., Int. Ed.* **2013**, *52*, 13580–13583.
- (21) Zhang, P.; Wang, M.; Li, C.; Li, X.; Dong, J.; Sun, L. Photochemical H₂ Production with Noble-Metal-Free Molecular Devices Comprising a Porphyrin Photosensitizer and a Cobaloxime Catalyst. *Chem. Commun.* **2009**, *46*, 8806–8808.
- (22) McCormick, T. M.; Han, Z.; Weinberg, D. J.; Brennessel, W. W.; Holland, P. L.; Eisenberg, R. Impact of Ligand Exchange in Hydrogen Production from Cobaloxime-Containing Photocatalytic Systems. *Inorg. Chem.* **2011**, *50*, 10660–10666.
- (23) Vagnini, M. T.; Smeigh, A. L.; Blakemore, J. D.; Eaton, S. W.; Schley, N. D.; D'Souza, F.; Crabtree, R. H.; Brudvig, G. W.; Co, D. T.; Wasielewski, M. R. Ultrafast Photodriven Intramolecular Electron Transfer from an Iridium-Based Water-Oxidation Catalyst to Perylene Diimide Derivatives. *Proc. Natl. Acad. Sci. U. S. A.* **2012**, *109*, 15651–15656.
- (24) Concepcion, J. J.; Jurss, J. W.; Hoertz, P. G.; Meyer, T. J. Catalytic and Surface-Electrocatalytic Water Oxidation by Redox Mediator–Catalyst Assemblies. *Angew. Chem., Int. Ed.* **2009**, *48*, 9473–9476.
- (25) Yamamoto, M.; Wang, L.; Li, F.; Fukushima, T.; Tanaka, K.; Sun, L.; Imahori, H. Visible Light-Driven Water Oxidation using a Covalently-Linked Molecular Catalyst-Sensitizer Dyad Assembled on a TiO₂ Electrode. *Chem. Sci.* **2016**, *7*, 1430–1439.
- (26) Duan, L.; Wang, L.; Li, F.; Li, F.; Sun, L. Highly Efficient Bioinspired Molecular Ru Water Oxidation Catalysts with Negatively Charged Backbone Ligands. *Acc. Chem. Res.* **2015**, *48*, 2084–2096.
- (27) Gao, Y.; Zhang, L.; Ding, X.; Sun, L. Artificial Photosynthesis-Functional Devices for Light Driven Water Splitting with Photoactive Anodes Based on Molecular Catalysts. *Phys. Chem. Chem. Phys.* **2014**, *16*, 12008–12013.
- (28) Duan, L.; Bozoglian, F.; Mandal, S.; Stewart, B.; Privalov, T.; Llobet, A.; Sun, L. A Molecular Ruthenium Catalyst with Water-Oxidation Activity Comparable to that of Photosystem II. *Nat. Chem.* **2012**, *4*, 418–423.
- (29) Duan, L.; Wang, L.; Inge, A. K.; Fischer, A.; Zou, X.; Sun, L. Insights into Ru-Based Molecular Water Oxidation Catalysts: Electronic and Noncovalent-Interaction Effects on Their Catalytic Activities. *Inorg. Chem.* **2013**, *52*, 7844–7852.
- (30) Knauf, R. R.; Kalanyan, B.; Parsons, G. N.; Dempsey, J. L. Shell Recombination Dynamics in Sensitized SnO₂/TiO₂ Core/Shell Photoanodes. *J. Phys. Chem. C* **2015**, *119*, 28353–28360.
- (31) Swierk, J. R.; McCool, N. S.; Nemes, C. T.; Mallouk, T. E.; Schmuttenmaer, C. A. Ultrafast Electron Injection Dynamics of Photoanodes for Water-Splitting Dye-Sensitized Photoelectrochemical Cells. *J. Phys. Chem. C* **2016**, *120*, 5940–5948.
- (32) Li, T.; Zhao, W.; Chen, Y.; Li, F.; Wang, C.; Tian, Y.; Fu, W. Photochemical, Electrochemical, and Photoelectrochemical Water Oxidation Catalyzed by Water-Soluble Mononuclear Ruthenium Complexes. *Chem. - Eur. J.* **2014**, *20*, 13957–13964.
- (33) Sherman, B. D.; Sheridan, M. V.; Dares, C. J.; Meyer, T. J. Two Electrode Collector–Generator Method for the Detection of Electrochemically or Photoelectrochemically Produced O₂. *Anal. Chem.* **2016**, *88*, 7076–7082.
- (34) Sheridan, M. V.; Sherman, B. D.; Fang, Z.; Wee, K. R.; Coggins, M. K.; Meyer, T. J. Electron Transfer Mediator Effects in the Oxidative Activation of a Ruthenium Dicarboxylate Water Oxidation Catalyst. *ACS Catal.* **2015**, *5*, 4404–4409.
- (35) Sherman, B. D.; Sheridan, M. V.; Wee, K. R.; Song, N.; Dares, C. J.; Fang, Z.; Tamaki, Y.; Nayak, A.; Meyer, T. J. Analysis of Homogeneous Water Oxidation Catalysis with Collector–Generator Cells. *Inorg. Chem.* **2016**, *55*, 512–517.
- (36) Ashford, D. L.; Sherman, B. D.; Binstead, R. A.; Templeton, J. L.; Meyer, T. J. Electro-assembly of a Chromophore-Catalyst Bilayer for Water Oxidation and Photocatalytic Water Splitting. *Angew. Chem.* **2015**, *127*, 4860–4863.
- (37) Sheridan, M. V.; Sherman, B. D.; Marquard, S. L.; Fang, Z.; Ashford, D. L.; Wee, K. R.; Gold, A. S.; Alibabaei, L.; Rudd, J. A.; Coggins, M. K.; Meyer, T. J. Electron Transfer Mediator Effects in Water Oxidation Catalysis by Solution and Surface-Bound Ruthenium Bpy-Dicarboxylate Complexes. *J. Phys. Chem. C* **2015**, *119*, 25420–25428.